# Excitation and Decay of Correlated Atomic States

A. R. P. Rau

Doubly excited states of atoms and ions in which two electrons are excited from the ground configuration display strong radial and angular electron correlations. They are prototypical examples of quantum-mechanical systems with strong coupling. Two distinguishing characteristics of these states are: (i) their organization into successive families, with only weak coupling between families, and (ii) a hierarchical nature of this coupling, with states from one family decaying primarily to those in the next lower family. A view of the pair of electrons as a single entity, with the electron-electron repulsion between them divided into an adiabatic and a nonadiabatic piece, accounts for many of the dominant features. The stronger, adiabatic part determines the family structure and the weaker, nonadiabatic part the excitation and decay between successive families. Similar considerations extend to three-electron atomic states, which group into five different classes. They are suggestive of composite models for quarks in elementary particle physics, which exhibit analogous groupings into families with a hierarchical arrangement of masses and electroweak decays.

Recent understanding of doubly and triply excited states of atoms is reviewed. New atomic developments highlight the occurrence of different families of multiply excited states, with decay between families weakened by a dynamical segregation of their wave functions into different regions of the full configuration space available to the electrons. Each family resides in the vicinity of one critical point of the system's potential. The resulting negligible overlap between the wave functions of distinct families leads to "almost good" quantum numbers (that is, those that appropriately describe the system) for labeling them and to selection rules governing transitions between them, all having a dynamical origin. Although not understood in their entirety, these features originate from the same basic (Coulomb) interaction that prevails between every pair of particles in the atom. The origin of these features may also be of interest elsewhere, for example, in particle physics, where analogous questions on the number of quark flavors, their origin, and associated masses are entirely open.

Excitation of a single, outer (valence) electron in a many-electron atom leads to a bound (Rydberg) state or to a continuum of ionized states with a residue left behind in its ground state. All these singly excited states, bound and continuum alike, may be regarded as a family of states built on the residue's ground state ($N = 1$), that is, the first ionization threshold of the atom, with the additional electron attached to it either in a discrete or in a continuum energy level. Doubly excited states of atoms involve the simultaneous excitation of two outer electrons. As with singly excited states built on $N = 1$, the doubly excited states can be organized into successive families built on excited states of the residue ($N = 2, 3, \ldots$) with the second electron attached in a discrete or continuum energy level with respect to the corresponding $N$th ionization threshold of the atom (*1, 2*).

In higher doubly excited states, the increasing liberation of both electrons from the dominant attractive Coulomb field of the rest of the atom (the "core") affords stronger correlations between the electrons. The structure, excitation, and decay of these three-body Coulomb systems (core + e + e)—and, indeed, even the appropriate basis and the very language for describing them—retain current interest as relevant evidence emerges from advanced experimentation (*3, 4*). Close analogies may be drawn between these atomic states and other few-particle phenomena in nuclear (*5*) and particle physics. The existence of a hierarchy among the families of successive doubly excited states, and of a hierarchical coupling that governs excitation and decay among them, finds counterparts in the particle physics hierarchy among the (three) families of quarks (*6*). Even the role played by the strong and the electroweak interactions for quarks parallels the atomic view of the Coulomb interaction between the three particles. A dominant part of this interaction describes the family structure of doubly excited states, and a weaker component governs the coupling between the families.

In this article I highlight analogies that speak to the unity of physics through a report of recent experimental data on the doubly excited states of $H^-$, the negative ion of hydrogen that is the prototypical two-electron system, and of their implications. An experimental echo of this unity is seen in the utilization of a high-energy beam of $H^-$, at a laboratory [Los Alamos Meson Physics Facility (LAMPF)] built for the study of elementary particles, to produce the latest and most extensive data (*3, 4*) on doubly excited states in $H^-$.

The author is in the Department of Physics and Astronomy, Louisiana State University, Baton Rouge, LA 70803.

## Families of Two-Electron States

The simplest two-electron atomic systems, He and $H^-$, serve as the prototypes for the study of double excitation; theory and experiment on these systems have provided most of our information on two-electron states (*2, 7*). Just as the understanding of the H atom as the prototype of one-electron atoms extends to singly excited states in all atoms, a thorough understanding of He and $H^-$ should transfer to doubly excited states in all atoms and molecules.

All the singly excited states of He can be considered as a family of states associated with $He^+$ ($N = 1$) and may be schematically represented by

$$\begin{pmatrix} He^+(N = 1) + e(\infty) \\ He(N = 1, n) \end{pmatrix} \qquad (1)$$

The top entry represents the continuum states with the electron at infinity with some kinetic energy; the bottom entry represents the bound states, with $n$ the principal quantum number of the excited electron. The kinetic energy and the quantum number $n$ are running indices so that each entry represents an infinite number of states. In spite of the infinity of states involved, their grouping into two, a top and a bottom entry, is instructive in spelling out the essential difference between these two groups and in drawing analogies to families of states elsewhere in physics. [In addition to the energy index, electrons also carry orbital and spin angular momentum so that there is one family for each ${}^{2S+1}L_J^{\pi}$ symmetry, where $\{S, L, J\}$ are the total spin, orbital, and combined angular momentum quantum numbers, and $\pi$ is the parity of the full three-body system. In the absence of coupling to external fields, these are, of course, good quantum numbers. From now on, we will generally deal with a single ${}^{2S+1}L_J^{\pi}$ set at a time.]

Doubly excited states may be described similarly as families associated with excited states $He^+(N)$ of the ion:

$$\begin{pmatrix} He^+(N = 2) + e(\infty) \\ He(N = 2, n) \end{pmatrix}, \begin{pmatrix} He^+(N = 3) + e(\infty) \\ He(N = 3, n) \end{pmatrix}, \ldots \qquad (2)$$

Because $He^+$, like H, has an infinite sequence of Bohr energy levels, there is an infinity of families in Eq. 2. Indeed, because of additional degeneracies of the Bohr levels, this is a multiple infinity of families of doubly excited states. The successive energies of $He^+(N)$ above the ground-state $He^+(N = 1)$ of the ion (which itself lies 24.6 eV above the ground state of the He atom) are given by the Bohr formula 4(13.6 eV) $(1 - 1/N^2)$. Although this description in terms of families in Eqs. 1 and 2 seems straightforward, arising naturally from the canonical language of atomic physics which deals with individual electrons, it is flawed in principle and fails particularly for the higher doubly excited states in Eq. 2. The Hamiltonian of a system of three particles with Coulomb interactions between each pair is nonseparable, rendering invalid the description in terms of individual electron quantum numbers.

The electron-electron interaction $e^2/r_{12}$, where $r_{12}$ is the interelectronic distance, makes the three-body Hamiltonian nonseparable. Only when it vanishes, or when its departure from the mean field of each electron is weak, is it meaningful to use an individual electron description. Thus, the top entries in Eqs. 1 and 2, wherein the two electrons separate mutually to infinity, are indeed meaningful and mark asymptotic states accessible to experiment. But the bottom entries in Eq. 2, or even for that matter in Eq. 1, are only approximately valid because of the $e^2/r_{12}$ potential. Indeed, this interaction mixes states of different families. The classification of these three-body states into families is inherently tied to the coupling between families that is responsible for their excitation and decay.

Even the very lowest doubly excited states in the first column of Eq. 2 exhibit a new decay mechanism not present for singly excited states in atoms. These doubly excited states are degenerate in energy with the singly excited continuum in Eq. 1, more energy being necessary to excite both electrons than to ionize a single one. Because of $e^2/r_{12}$, energy eigenstates are linear combinations of the two degenerate types, causing discrete states in $He(N = 2, n)$ to decay into $He^+(N = 1) + e(\infty)$, a process called autoionization (8). Therefore, unlike the singly excited bound states in the bottom entry in Eq. 1, the states in the bottom entries in Eq. 2 represent only quasi-bound states, with finite autoionization lifetimes and energy widths. This physical process of autoionization decay (9) is inherent to the three-body system and to its "internal" Hamiltonian (specifically, its $e^2/r_{12}$ term) and exists even in the absence of coupling to the radiation field. Coupling to that field leads to additional radiative decays involving changes in $\{S, L, J, \pi\}$ to conform to dipole selection rules, whereas these quantum numbers remain unchanged in autoionization.

Rewriting Eqs. 1 and 2 for the very similar system of $H^-$ and displaying also the possible transitions between families, I sketch schematically in Fig. 1 the realm of two-electron atomic physics. Dashed arrows represent electron ejection in autoionization, one electron dropping down to a more bound level and giving the energy thus gained to its partner, which is then able to escape to infinity. Wavy arrows represent photon emission from doubly excited states of $H^-$ to lower doubly excited or to singly excited states. Photon emission is also possible at fixed $N$ and is represented by a dotted line in the figure. Each of the lower entries in Eqs. 1 or 2 represents infinitely many states; a state with higher energy can radiatively decay to another with lower energy with, of course, attendant changes in $\{L, J, \pi\}$. Reversing the arrows would describe excitation of doubly excited states, either by electron impact on H or by photoabsorption from the ground state of $H^-$.

One can make an instructive analogy with families of quarks and leptons and the standard model of electroweak interactions (*10*). Here we have three families of leptons and, correspondingly, three of quarks, generally grouped into doublets as in Fig. 2. Leptons participate only in electroweak interactions, whereas the quarks have, in addition, the strong interaction. Indeed, this is the dominant interaction that determines their masses and other gross structure. Therefore, the physical doublets involve the so-called primed quarks d′, s′, and b′ that are related to the unprimed quarks through the Kobayashi-Maskawa (KM) matrix [(*11*, *12*); S43 and appendix III of (*10*)]:

$$\begin{pmatrix} d' \\ s' \\ b' \end{pmatrix} = \begin{pmatrix} V_{ud} & V_{us} & V_{ub} \\ V_{cd} & V_{cs} & V_{cb} \\ V_{td} & V_{ts} & V_{tb} \end{pmatrix} \begin{pmatrix} d \\ s \\ b \end{pmatrix} \quad (3)$$

where $V_{ij}$ are the weak charge-changing interaction elements between particles $i$ and $j$, and the subscripts refer to the various quarks: u, up quark; d, down quark; t, top quark; b, bottom quark; c, charmed quark; and s, strange quark. This matrix has diagonal elements $\simeq 1$ and small off-diagonal elements, reflecting the relative dominance of strong interactions over the others. But the off-diagonality is important, permitting decays not only within individual families but also between families, albeit weaker in strength. In Fig. 2, charged current decays are shown as dashed lines and neutral ones as dotted or wavy lines in analogy with Fig. 1. In this analogy between atomic and quark families, charged current decays correspond to autoionization (a negative electron emitted) and neutral currents to radiative decays. Flavor-changing neutral currents (wavy lines in Fig. 2) seem to be suppressed, the only neutral currents that have been observed being ones involving the same quark (dotted lines in Fig. 2). In the parallel atomic example in Fig. 1, autoionization decays generally dominate (by several orders of magnitude) over radiative decays in light atoms.

It is intriguing to stretch this analogy even further in one regard. For the atomic families in Eqs. 1 and 2, both the top and bottom entries would indicate exact energy eigenstates if the $e^2/r_{12}$ interaction were switched off. Then the independent electron quantum numbers such as $N$ and $n$ (and their individual angular momentum labels) would be good quantum numbers. When this interaction is turned on, these quantum numbers lose their validity. How-

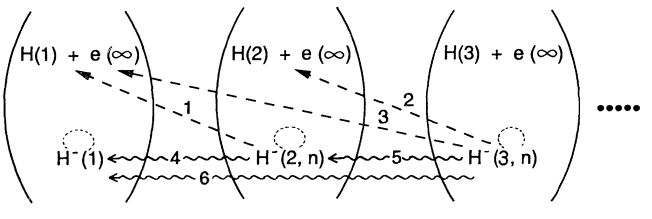


**Fig. 1.** States of the $(H^+ + e + e)$ system organized into families associated with the H($N$) states of $(H^+ + e)$, $N = 1, 2, 3, \ldots$. The top entry in each family represents an infinity of continuum states, the bottom entry an infinity of discrete energy levels. Dashed arrows show autoionization decays, accompanied by ejection of an electron; wavy arrows and dotted lines show radiative decays.

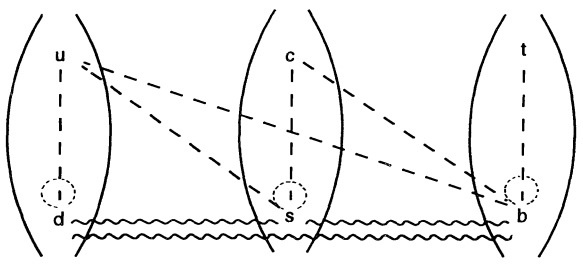


**Fig. 2.** The three families of quark-doublets with charged (------) and neutral (. . . . . .) current decays shown. Flavor-changing neutral currents (~~~~) seem to be suppressed.

ever, the upper entries in the families remain physically meaningful—identified, in fact, by an experimental arrangement that detects the electron at infinity together with the state of excitation of the residue—whereas the lower entries are now no longer eigenstates. The difference lies in that, for the top entries, the two electrons are separated to infinity where $e^2/r_{12}$ vanishes, whereas for the bottom entries $r_{12}$ is finite, thus invalidating the independent electron labels. Bottom entries drawn from different families in Eq. 2 that share the same {$S$, $L$, $J$, $\pi$} but differ only in $N$ and $n$ are mixed by the electron-electron interaction with the result that the physical eigenstates are linear combinations of various independent particle configurations. (Incidentally, only the nonseparable portion of the interaction is responsible for this mixing and therefore for the contrast between top and bottom entries.) Turning to the quark families, we see again that the top members are unchanged (this is a standard choice), only the bottom ones getting mixed as in Eq. 3 upon the superposition of electroweak and strong interactions. The analogy may suggest a dynamical explanation in terms of an underlying substructure of quarks ("ur-quarks"?). Suppose, as in the atomic example of three charged particles, the quarks themselves are composites of three ur-quarks. A distinction can then be made between two types of composites of the three ur-quarks, depending on whether one pair of relative distances vanishes (recall an inversion in the nature of chromodynamics relative to electrodynamics, that the interaction vanishes when distances go to zero rather than to infinity). One type, with a pair of ur-quarks having zero separation, would correspond to the u, c, and t, while a second, in which all pairs are finitely separated, to the d, s, and b. In the language of atomic physics, the switching on of interactions between the ur-quarks causes "configuration mixing" of the d, s, and b as given by the KM matrix in Eq. 3.

## Experimental Data on Doubly Excited Atoms

This section gives a brief review of experiments on doubly excited states over the last 20 years. It is designed to highlight those key features of the data that will be picked up in the next section to draw lessons on the family structure and on the hierarchical coupling between families of states of the three-body atomic system.

*Excitation by photons.* The simple sketch in Fig. 1 of two-electron states also shows how they may be excited and observed in the laboratory. One method is photoabsorption from the ground state of $H^-$, or He, in an energy range below the detachment or ionization thresholds H($N$) or $He^+(N)$. Against the background of the absorption into the one-electron continuum of the first family, structures appear in the absorption cross section at specific energies marking the positions of doubly excited states. The first doubly excited states in atoms were observed in this way in He (*13*), utilizing synchrotron light from electron synchrotrons that provide photons of the requisite energy (≃60 eV or 20 nm). States of $^1P_1{}^0$ symmetry of the $N = 2$ family in Eq. 2 were observed as a Rydberg sequence of resonances converging to the $He^+(N = 2)$ limit, which lies 24.6 + 54.4(1 − 1/4) = 65.4 eV above the ground state of He. Experiments with synchrotron light in many other atoms have since been designed to study such sequences of doubly excited states, typically with relatively small values of $N$ (*14*). The most recent data (*15*) through $N = 6$ are shown in Fig. 3. States of much larger $N$ have not been observed. This is not because of any lack of photon energy in synchrotron sources but more a reflection of the weakness of excitation to such $N$ as will be discussed.

Lasers provide much higher resolution, and stepwise absorption of multiple laser photons has reached doubly excited states in more complex atoms, particularly in the alkaline earths such as barium. However, the lowest quasi-bound states within a family when $N$ is large have remained out of reach. As typical examples, when $N$ is 4 or 5, the states observed can be attributed to principal quantum numbers $n$ larger than 10 for the second electron (*16*), or, when $N$ is 20, the values of $n$ are 40 or larger (*17*). That is, the doubly excited states of high excitation that have been studied through multiple laser photoabsorption have a very unequal energy sharing between the two electrons. States in which the two electrons have comparable radial excitation, which are the lowest members of each column in Eq. 2 or in Fig. 1, have remained elusive to such laser experimental searches, the best results being those in (*18*).

The longest sequence of comparably excited states seen in photoabsorption is from a very recent study on $H^-$ at LAMPF (*3*, *4*). (In such particle physics laboratories, $H^-$ is often the initial charged species that is accelerated. Later, upon stripping of the two electrons, proton beams and subsidiary meson or neutrino beams are generated.) In a very innovative use of the relativistic beam of $H^-$ (≃800 MeV) for atomic physics studies, Howard Bryant and his colleagues have studied various aspects of this atomic negative ion (*19*). The recent ex-

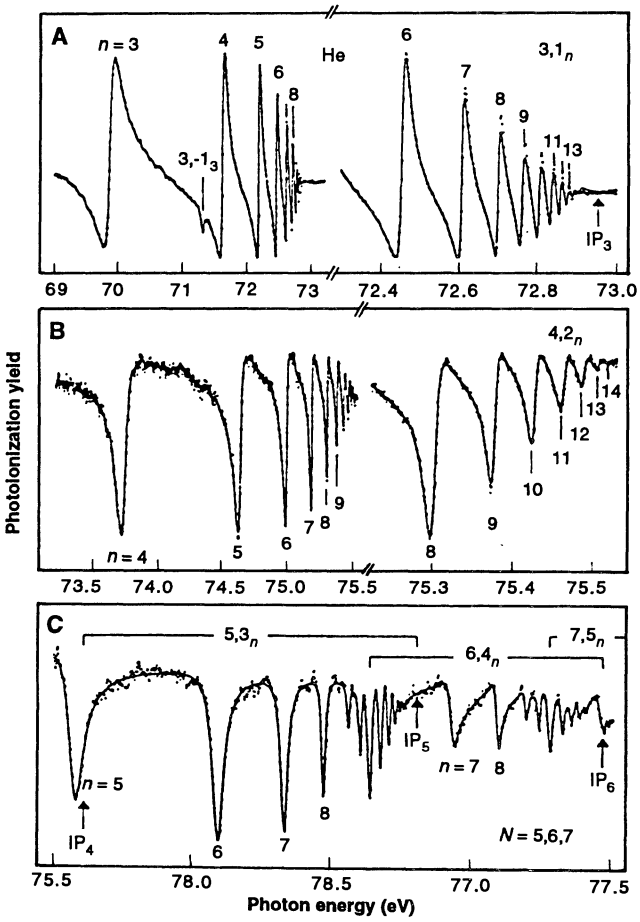


**Fig. 3.** (**A**) He($N$ = 3, $n$), (**B**) He($N$ = 4, $n$), and (**C**) He($N$ = 5, $n$) and He($N$ = 6, $n$) $^1P^0$ doubly excited states seen in photoabsorption with synchrotron light. Panels (A) and (B) include on the right a magnified high $n$ region. [From (*15*), with permission]

periment (*3*, *4*) measured photodetachment by a laser photon through $^1P_1{}^0$ doubly excited states of the $N = 6$ and 7 families. Earlier experiments had already observed the $N = 2$ and 3 states. The required photon energy of ≃14 eV was achieved by using the relativistic Doppler effect. The fourth harmonic of a yttrium-aluminum-garnet (YAG) laser with laboratory photon energy of ≃4 eV appears in the frame of the relativistically moving negative ion as higher in energy by a factor of 3 to 4 depending on the angle between the laser and $H^-$ beams. The maximum enhancement occurs by shining the laser beam head-on at the negative ion beam. By changing the angle in a controlled fashion, the effective photon energy can be tuned continuously up to about 16 eV (otherwise inaccessible to tunable laboratory laser sources), with resolutions that can surpass 10 meV. Figure 4 shows the latest data for the $N = 6$ family. Note again sequences of resonances, seen as fairly narrow dips in the cross section. The experiment monitors the neutral, excited H atom in various stages of excitation, H($N$). With reference to Fig. 1, states of, say, $H^-(N = 3, n)$ formed on photoabsorption from the $H^-$ ground state (along path 6 with reversed arrow) autoionize along paths 2 or 3 to H(2) and H(1), respectively, and may therefore be observed in either of these channels by the H($N$) detector. A crucial result of these and other experiments is that the states of a certain $H^-(N, n)$ are best observed in the H($N - 1$) channel, suggesting that the decay between families proceeds preferentially to the next lower one (*4*).

*Excitation by charged particle impact.* Doubly excited states have also been studied in electron collisions with atoms and ions. Consider (Fig. 1) elastic scattering of electrons from H in the ground state. At energies of ~10 eV where these elastic scattering states in the top of the first column are degenerate with $H^-(N = 2, n)$ states in the second column, such doubly excited states will be excited (along path 1 with reversed arrow) and subsequently de-excited (path 1) back to the elastic channel. The doubly excited states appear as resonances in the elastic scattering cross section. The resonances are sharp, reflecting the weakness of coupling. At higher energies, doubly excited states of higher families will be observed similarly (excitation and de-excitation along path 3, for example). The higher states such as $H^-(N = 3, n)$ may be excited along path 3 and then decay not by path 3 but by path 2 to an excited continuum. The doubly excited $H^-(N = 3, n)$ states can therefore also be observed in the inelastic scattering cross section, e + H($N = 1$) → e + H($N = 2$). Experiments with He being simpler than with atomic hydrogen, the very first observation of doubly excited states was in elastic e + He scattering (*20*). (Although these doubly excited states belong to the three-electron $He^-$ system, only two electrons are excited in an appropriate energy range. The first excited state in He lies at 20.2 eV and the first ionization potential at 24.6 eV, so that for e + He collisions in the incident energy range from 19 to 25 eV only two electrons are actively involved, the third remaining as a spectator in the ground state.) The most recent of such data (up to $N = 9$) have been obtained in inelastic scattering in this energy range (*21*).

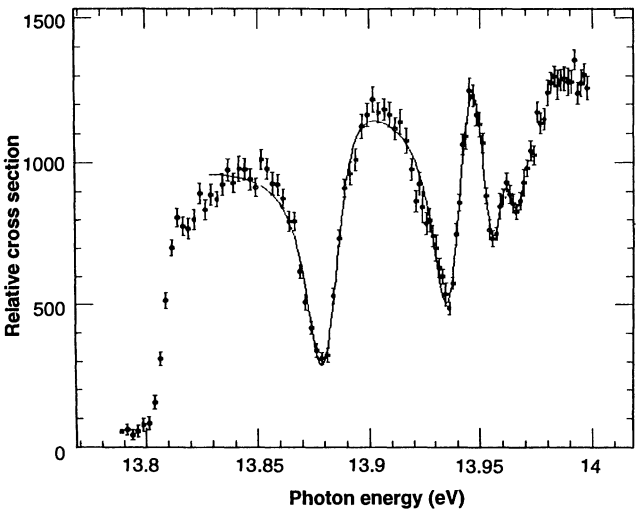


**Fig. 4.** $H^-(N = 6, n)$ resonances seen in the photodetachment $h\nu + H^- \rightarrow H(N = 5) + e$. [From (*3*), with permission]

Doubly excited states can also be reached by impact of heavier charged particles on atoms (*22*, *23*). Indeed, such slow collisions between two atomic systems, both carrying a complement of electrons, may well be the preferred route to high doubly excited states. But, in view of the very large density of states, judicious detection schemes may be necessary to sort out the resulting complex spectrum.

## Excitation, Decay, and Structure of Two-Electron States

*Key features of the data on doubly excited states.* The brief survey of experimental data in the previous section provides major clues to the nature of doubly excited states. First, the very observation that data on higher families are extremely limited seems innocent but has an important implication. For all the effort over 25 years by various experimental groups and with the use of various techniques, long family sequences have only been observed in $H^-$ and $He^-$ and even then only up to $N < 10$. Considering that $N$ could rise to ∞, and that all atoms and negative ions have such doubly excited states, this paucity of data is indeed remarkable. It points to the low probability for exciting such states starting from ground states of atoms and ions. A close corollary is that the linewidth of these states is very narrow, particularly with increasing $N$. Even leaving aside certain almost stable states (*24*) with special selection rules for $\{S, L, J, \pi\}$, nearly all doubly excited states are remarkably sharp and consequently long-lived, as seen in Figs. 3 and 4. Considering how high in energy they lie, with even the lowest ($N = 2$, $n \simeq 2$) state in Eq. 2 or in Fig. 1 accessing infinitely many singly excited states that lie lower in energy, such long lifetimes are again remarkable. In an analogous situation, when the first charmonium bound states were experimentally observed, the particle physics community was astonished at the narrowness of these levels at such high energies. This result was then attributed to a new quantum number, charm, and to its conservation. The corresponding situation with doubly excited states is explained on dynamical grounds; clearly, three-body dynamics leads to almost good quantum numbers and astonishing selection rules (which render pathways such as 1, 2, and 3 in Fig. 1 weak) without any obvious correspondence to an underlying symmetry.

The weakness of excitation and the stability against decay are, of course, closely related, having the same origin. As will be discussed below, the wave functions of many doubly excited states are concentrated into limited regions of space, very different from those of the wave functions of most other states, particularly of singly excited states. This implies small overlaps between single and double excitations.

Another major feature of the experimental data is the hierarchical nature of the decay between families. When, for instance, both paths 2 and 3 (Fig. 1) are possible, the former transition is stronger. A similar observation has been made regarding the quark families in Fig. 2. Thus, b → c transitions dominate over b → u,

experimental measurements suggesting $|V_{ub}|/|V_{cb}| \simeq 0.1$ [(25), section IV B of (12)]. A full explanation for this hierarchical nature of the coupling between families has not been provided in either system.

*Role of the electron-electron interaction.* In the case of quarks, the weakness of the coupling between families is attributed directly to the strengths of the basic interactions, electroweak interactions being inherently weaker than strong interactions. For the three-body atomic system, there is only one interaction between the two electrons, namely, the Coulomb interaction $e^2/r_{12}$. In its absence, the problem would be separable and each family in Eq. 2 or in Fig. 1 would be distinct, with no transitions between them. The $e^2/r_{12}$ interaction invalidates the independent or individual electron description behind Fig. 1. In describing a doubly excited state of a given $^{2S+1}L_J^{\pi}$ symmetry, all independent-electron configurations that share the same $\{S, L, J, \pi\}$ are in principle mixed by $e^2/r_{12}$.

Diagonalization of the $e^2/r_{12}$ matrix over all these configurations yields the energy eigenstates, but its dimension is multiply infinite because of the nature of Coulomb spectra. Conventional atomic structure calculations, carried out through one or another technique to describe this configuration mixing by retaining a large number of basis states, have provided much useful information on the lower doubly excited states (26–28), particularly with judicious selections of basis states (29). Their deficiency lies on the practical side in becoming prohibitively cumbersome numerically, particularly as $N$ is increased, because of the necessity to superpose an explosively large basis. Semiclassical quantization schemes based on trajectories calculated through classical mechanics have also been used but also only at relatively low $N$ (30). We turn, therefore, to models that focus on two-electron basis functions from the start.

Here again, an analogy with quark families is instructive. The two features, the existence of families determined in the main by strong interactions and the weak couplings between them due to electroweak interactions, have a natural correspondence with the hierarchy of interaction strengths. In the atomic problem we have a single unified interaction $e^2/r_{12}$. To sift out the two features sketched in Fig. 1, we need to divide this interaction into two pieces, of which a dominant one (the separable part of $e^2/r_{12}$ in combination with the single electron–nucleus attraction) determines the family structure and a secondary (nonseparable) one the excitations and decays between them. Note the irony in contrasting the two fields, because the current quest in particle physics is in the opposite direction, to put both strong and electroweak interactions and all the particles into a unified whole.

The subdivision of $e^2/r_{12}$ into two pieces takes cues from molecular structure where an adiabatic separation is made between the more energetic electronic motion and a slower motion of the nuclei. A similar treatment of the full three-body atomic interaction, with an adiabatic separation of the radial size from the coordinates that describe radial and angular correlation, organizes states into families in Fig. 1, whereas residual, nonadiabatic couplings between the size and the correlations account for their excitation and decay.

*A molecular orbital model.* Two different procedures that exploit the molecular analogy have been used in our current understanding of doubly excited states. One, which has come later and has been pursued only very recently (31–33), is to make a 1:1 correspondence between the states of $H_2^+$ and of $H^-$, which differ in the relative masses of the pair of identically charged particles to the third one of opposite charge [see also (34)]. With $r_{12}$ playing the role in $H^-$ that the internuclear coordinate $R$ does in $H_2^+$, the familiar Born-Oppenheimer potential curves $U(R)$ have been translated into the $H^-$ system (33). In the adiabatic handling of this coordinate, the system separates in prolate spheroidal coordinates and three quantum numbers $n_\lambda$, $n_\mu$, and $m$ label the molecular orbitals, representing, respectively, the numbers of ellipsoidal, hyperboloidal, and azimuthal nodes of the wave function. Each molecular orbital's potential curve $U(R)$ supports a family of bound and continuum states identified with the families in Fig. 1. In the "united atom" limit where $R \to 0$, for $H^-$ these quantum numbers reduce to the spherical quantum numbers $n\ell m$. In the "separated atom" limit of $R \to \infty$, where one electron is far from H, they reduce instead to the parabolic quantum numbers that are relevant to the Stark effect in H, where the electric field originates from the far-away electron (35).

The Born-Oppenheimer adiabatic separation for molecules of the internuclear coordinate $R$ from the electronic coordinate $r$ (with respect to the center-of-mass of the two protons in $H_2^+$) is, of course, approximate, the full Hamiltonian not being exactly separable. There remain residual nonadiabatic couplings between the different molecular orbital potential curves, usually concentrated near curve crossings of two of these curves. These nonadiabatic couplings lead to molecular dissociation. In the translation to $H^-$, it is these nonadiabatic couplings that lead to autoionization decays in Fig. 1 (32). Even and odd values of $n_\mu$ correspond to even or odd wave functions under interchange of the two electrons. The former, concentrated in a spatial configuration with the nucleus midway between the electrons, characterizes doubly excited states with comparable radial excitation of the electrons. Potential curve crossings involving such even $n_\mu$ show stronger couplings. Families with even or odd $n_\mu$ couple among themselves, and the decay of states with either symmetry occurs preferentially at the crossing to the next lower molecular orbital with $n_\mu$ smaller by 2. Because the ground state of $H^-$ has $n_\mu = 0$, the dominant excitation of a single set of doubly excited resonances below each $H(N)$ and the hierarchical nature of the decay between the two families find explanation in the symmetry with respect to the $n_\mu$ quantum number (36).

*A hyperspherical coordinate model for the two-electron system.* Although the above molecular orbital model has attractive features, there is no basic explanation for the adiabatic separation between the interelectronic coordinate and the position of the nucleus with respect to their center of mass. In the Born-Oppenheimer treatment of molecules, adiabatic separation of nuclear and electronic motion is naturally explained by the small mass ratio of electrons to nuclei. No such immediate explanation in terms of a small parameter is available for doubly excited states of $H^-$ or other atoms. We turn, therefore, to another model that has been explored now for 20 years (7, 37, 38) without invoking from the start an analogy to molecular structure, but nevertheless paralleling the molecular analog. This model also contains a division of the interaction into an adiabatic piece that sets the family structure and a nonadiabatic coupling that leads to the weak decays between them. The two pieces are, however, now associated, respectively, with strong correlations between the electrons and with the overall size of the three-body system.

Instead of the position vectors $\mathbf{r}_1$ and $\mathbf{r}_2$ of the two electrons with respect to the (infinitely) massive nucleus, joint or pair coordinates are introduced (39):

$$R = (r_1^2 + r_2^2)^{1/2},$$

$$\alpha = \arctan(r_2/r_1),$$

$$\theta_{12} = \arccos(\hat{r}_1 \cdot \hat{r}_2) \qquad (4)$$

In this "hyperspherical" coordinate system, the six coordinates of the full three-body system describe a six-dimensional hypersphere, whose radius $R$ indexes the overall size of the system. The two "dynamical" angles, $\alpha$ and $\theta_{12}$, out of the five angular coordinates (the other three being Euler angles that do not enter into the potential energy of the system) naturally describe radial and angular correlations, respectively, of the two electrons. A significant fea-

ture of all two-electron state wave functions, whether calculated through conventional independent-particle configuration mixing or through the hyperspherical procedure described below, is that they divide into two classes (*40*). One concentrates about $\alpha \simeq \pi/4$, which corresponds to equal radial excitation, the other about $\alpha \simeq 0$ or $\pi/2$, both concentrations sharpening with increasing excitation. The importance of the concentration at $\alpha \simeq \pi/4$ had actually been pointed out for two-electron continuum functions near threshold, which govern the escape of two electrons from a positive ion (*41*). High doubly excited states with comparable excitation are natural adjuncts to the double escape on the discrete side.

The two-electron Schrödinger equation remains nonseparable in hyperspherical coordinates. Adiabatic separation of $R$ from the angular coordinates $\alpha$ and $\theta_{12}$ successfully describes at least the lower families in Fig. 1. At each fixed $R$, the Schrödinger equation is solved to give eigenvalues $U(R)$ and eigenfunctions $\phi(R; \alpha, \theta_{12})$ that depend parametrically on the "slow" coordinate $R$ (*37, 38*). As in the Born-Oppenheimer treatment of molecules, treating each $U(R)$ as an independent potential well supporting a family of bound and continuum states amounts to an adiabatic approximation and provides the families in Fig. 1.

In the adiabatic hyperspherical scheme, the adiabatic (nonadiabatic) decomposition of $e^2/r_{12}$ to give family structure (excitation and decay between families) reflects a faster motion in the angles $\alpha$ and $\theta_{12}$ relative to a slower motion in $R$. That is, radial and angular correlations between the electrons develop faster than an overall size scaling of the three-body system. This is plausible on many grounds, particularly with increasing excitation, because the two slow electrons are then further removed from the core's attraction, allowing strong correlations to develop between them. However, no simple parameter, such as the ratio of electronic to nuclear mass in the case of molecular spectra, is available to index the amount of nonadiabaticity in this description of $e^2/r_{12}$ for two-electron states.

Figure 5 shows a series of $^1P^0$ potential curves for the $H^-$ system (*42*). One dominant potential well converges at large $R$ to each H($N$) state, depending asymptotically on the dipole potential of the e + H($N$) system (*43*). Each well supports a sequence of bound states (*44*). The experimentally observed (*3, 4*) series of quasi-bound states in each family, such as the ones in Fig. 4 for $N = 6$, are well described by these calculated dipole-bound states (*42, 45*). Only one dominant series is observed with wave functions symmetric under radial interchange $r_1 \leftrightarrow r_2$ [which translates into $\alpha \rightarrow (\pi/2) - \alpha$] and substantially concentrated at $\alpha \simeq \pi/4$ (equal radial excitation). Just as with the similar discussion with respect to $n_\mu$ in the molecular orbital model, the excitation and decay between families seem to proceed mainly within this subclass of states. Along with the tight radial correlation implied by the concentration at $r_2/r_1 \simeq 1$, these states also display a strong angular correlation with wave functions concentrated at $\theta_{12} \simeq \pi$.

The point $\alpha = \pi/4$, $\theta_{12} = \pi$ is a saddle point of the potential in the three-body Coulomb system (*7*) and is the seat of the dominant class of states. The wave functions of this class overlap little with those of other—particularly singly excited—states, whose functions are concentrated in the potential valleys at $\alpha \simeq 0$ and $\pi/2$. Small overlap with singly excited states (particularly with the ground state) makes for small excitations. The conclusion is immediate for direct photoabsorption from the ground state. For slow electron impact, one might envisage excitation to the higher wells in Fig. 5 through the stepwise ladder provided by the lower wells, but this mechanism also becomes inefficient with increasing $N$ (*21*). States in successive wells are staggered in $R$, so that their overlap is again ordered hierarchically. (In molecular physics, these overlaps are termed Franck-Condon factors.) The nonadiabatic coupling between potential curves is only strong near their avoided crossings, which occur at larger $R$ as $N$ increases (Fig. 5). Given the Coulomb scaling in $1/R$, these couplings become weaker, making the high $N$ states difficult to access. These same features, namely, hierarchical ordering in the overlap between the states in different wells and weak couplings, account for the preferential decay of $H^-(N, n)$ states into the continuum in the $N - 1$ potential well (*45, 46*).

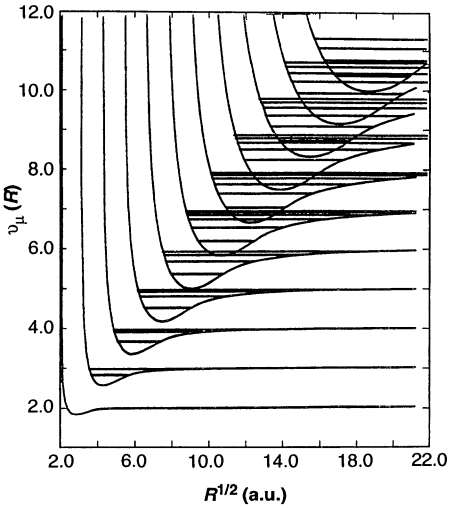


**Fig. 5.** Lowest potential curve in $^1P^0$ symmetry of $H^-$ in the adiabatic hyperspherical model converging to each H($N$) threshold shown as effective quantum numbers $\nu = [-U(R)/13.6\ \text{eV}]^{-1/2}$ plotted against the square root of the hyperspherical radius $R$ defined in Eq. 4 (a.u., atomic unit); $\nu$ converges asymptotically to $N$. Positions of discrete energy eigenvalues in each potential are shown by horizontal lines. [From (*42*), with permission]

All the doubly excited state resonances observed in experiments such as in Figs. 3 and 4, or in the theoretical calculations of Fig. 5, can be capsuled into a single energy expression with two components (*42*). One component makes successive $n$ levels within each family depend only on the relevant dipole strength. The second component provides the link between families through a pair-Rydberg formula for the lowest levels of each $N$ (*47*). These lowest members of each family in Fig. 1 can be described without reference to any single-electron features (such as in the asymptotic description of the hyperspherical potential curves). Throughout, the three-body system can be viewed as a whole, namely, as a pair (*48*) of electrons attached to the positive core (called the "grandparent," namely, the bare $H^+$ or $He^{2+}$ in the two systems we have considered), with pair coordinates and corresponding quantum numbers and a pair-Rydberg expression that has the double-ionization threshold as its limit (*40*). This picture organizes the states in a very different way from that of Fig. 1, whose families converge to single-ionization ("parent") limits. Its levels fit into a single description with the full potential taken into account, breakdown into families, and decays between them arising only upon consideration of single-electron asymptotic states H($N$) + e($\infty$) with the attendant splitting of the full interaction $e^2/r_{12}$ into (dominant) adiabatic and (weak) nonadiabatic pieces.

The unification of all two-electron states with finite $R$ (and, therefore, finite $r_{12}$) in a single pair picture is the counterpart of the grand unified theory of strong and electroweak interactions. Subdivisions into family structures and coupling between them arise only upon departing from the unified view and upon splitting what is a unified whole into subgroups: strong (electroweak) or adiabatic (nonadiabatic) pieces of $e^2/r_{12}$, respectively. The existence of classes of states, such as the valley and saddle states, with little mutual overlap, is also likely to be of wide relevance to few-body problems in physics, including the one for ur-quarks mentioned earlier and for three-electron atomic states to which we will turn in the next section. In fact, with increasing number of variables, saddles (of different "flavors") proliferate in the listing of extremal points of a many-dimensional space.

**Table 1.** The three kinds of critical points, their definition in terms of the values of $\alpha$ and $\theta_{12}$ along with the local variation [whether maximum (max) or minimum (min)] of the potential around them, and the corresponding configurations for a positive core and two electrons. The fourth column gives the specification in terms of the coordinates $\mathbf{r}_1$ and $\mathbf{r}_2$ of the two electrons with respect to the core. Parentheses in the last column represent a close cluster of two particles.

| $\alpha$ | $\theta_{12}$ | Critical point | Values of $r$ | Configuration |
|---|---|---|---|---|
| $\pi/4$, max | 0, max | Peak | $\mathbf{r}_1 = \mathbf{r}_2$ | +(ee) |
| $\pi/4$, max | $\pi$, min | Saddle | $\mathbf{r}_1 = -\mathbf{r}_2$ | e+e |
| 0, min | | Valley | $\mathbf{r}_1 \simeq 0$ | (+e)e |

## Three-Electron States and Quark Analogs

As developed in the above section, the study of two-electron states in atoms points to the existence of two types of doubly excited states, valley and saddle. The corresponding wave functions are concentrated in the valleys and saddle of the total potential, which is the sum of the two Coulomb attractions between the core and the electrons and of the Coulomb repulsion between the electrons. In terms of the hyperspherical coordinates defined in Eq. 4, $R$ is a scale factor common to all three terms. The significant structure of the potential lies, therefore, in the dependence at any fixed $R$ on the two variables $\alpha$ and $\theta_{12}$. The values $\theta_{12} = 0, 2\pi$ lead to maximum, and the value $\theta_{12} = \pi$ to minimum, repulsion. In the variable $\alpha$, the potential exhibits deep (infinite) minima at $\alpha = 0, \pi/2$, corresponding to one or the other electron collapsing onto the core. The critical points of the potential can, therefore, be enumerated as in Table 1. Apart from the peak at $\alpha = \pi/4$ and $\theta_{12} = 0$ (that is, $\mathbf{r}_1 = \mathbf{r}_2$, such a coincident position of two electrons leading to infinite repulsion) that does not support any stable states, the other two extremal points support the two classes of states that are observed.

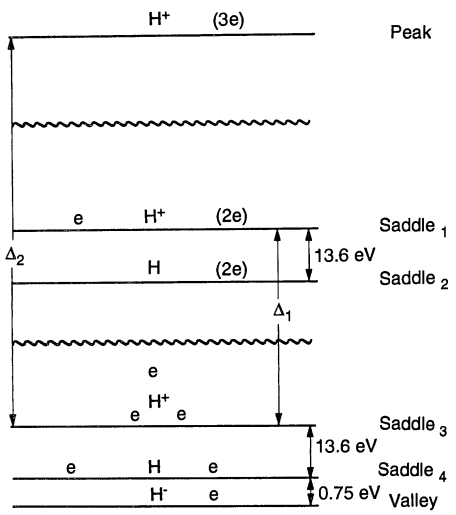


**Fig. 6.** Sketch of the relative energies of the six types of states listed in Table 2 for a system consisting of a proton and three electrons. Note two breaks in the energy scale corresponding to uncontrolled parameters $\Delta_1$ and $\Delta_2$, which represent, respectively, the large positive repulsive energies when two or three electrons cluster together.

**Table 2.** Similar to Table 1 but for a core plus three electrons. The first two columns define the nature of the critical points in terms of the local variation of the potential with respect to the two radial-correlation coordinates $\alpha_1$ and $\alpha_2$ and the three angles between the radial vectors of the electrons, $\theta_{ij}$. The fourth column gives the definition in terms of the values of $\mathbf{r}_1$, $\mathbf{r}_2$, and $\mathbf{r}_3$, which lie in a plane and with fixed $R = (r_1^2 + r_2^2 + r_3^2)^{1/2}$. In the corresponding sketch of the configurations in the last column, parentheses enclose clusters of particles. See also Fig. 6.

| $\alpha_1$, $\alpha_2$ | $\theta_{ij}$ | Critical point | Values of $r$ | Configuration |
|---|---|---|---|---|
| max in both | max in all three | Peak | $\mathbf{r}_1 = \mathbf{r}_2 = \mathbf{r}_3$ | +(eee) |
| max in both | max in one, min in two | $\text{Saddle}_1$ | $\mathbf{r}_1 = \mathbf{r}_2 = -\mathbf{r}_3$ | e+(ee) |
| max in both | min in all three | $\text{Saddle}_3$ | $r_1 = r_2 = r_3$, $\theta_{ij} = 120°$ | e / + / e e |
| max in one, min in other | max in one | $\text{Saddle}_2$ | $r_1 \simeq 0$, $\mathbf{r}_2 = \mathbf{r}_3$ | (+e)(ee) |
| max in one, min in other | min in one | $\text{Saddle}_4$ | $r_1 \simeq 0$, $\mathbf{r}_2 = -\mathbf{r}_3$ | e(+e)e |
| min in both | | Valley | $r_1 \simeq 0$, $r_2 \simeq 0$ | (+ee)e |

If we turn to the three-electron system, Table 2 enumerates the similar but richer variety of critical points of the potential, which now consists of six Coulomb interactions and, correspondingly, five dynamical coordinates, $\alpha_1$, $\alpha_2$, $\theta_{12}$, $\theta_{23}$, and $\theta_{31}$. Detailed definition is unnecessary here [see section 10.7 of (7)] but suffice it to say that, besides the valleys (two electrons close to the core) and peak (all three electrons coincident), there are four types of saddles. The table shows the physical configuration associated with each. In particular, the saddle point defined by the configuration in which the three electrons lie at vertices of an equilateral triangle with the core at the center is the seat of states that dominate near the threshold for three-electron escape from a positive charge [section 10.7.4 of (7)]. The different saddles lie at successively higher energies above the valley, and Fig. 6 provides the relative energy positions of various classes of three-electron states.

The above picture suggests a simple model for quarks, accounting for their number and relative energies (masses). Imagine a substructure for these particles with each quark made up of a triplet of "ur-quarks," which are themselves spin-1/2 objects just as are the quarks [see also (6)]. We can envisage pairwise interactions (albeit different from Coulomb) between them as well as one-particle energies for each ur-quark (stemming, for instance, from a pressure inside a confining "bag"). In this way, a correspondence can be set up between the states formed by triplets of ur-quarks held inside a bag and the three-electron states in Fig. 6. The different flavors of quarks would be associated with concentration of the ur-quark wave function in the different saddles and valleys of a common unified potential, providing a dynamical origin for the flavor symmetry. The electroweak coupling between different flavors would be seen as the weak residual remnant of the unified interaction and thereby the counterpart of the nonadiabatic, nonseparable piece of $e^2/r_{12}$ that is responsible for transitions between the six different arrangements shown in Fig. 6 for three-electron atoms.

It is interesting that, in the atomic example, the relative energies can be fixed for the most part but for two "uncontrolled" parameters $\Delta_1$ and $\Delta_2$ representing the large repulsion when either two or all three electrons coincide. As a result, one can accommodate in this picture the sixth and highest state being arbitrarily higher in energy than the others with obvious implications for either a very heavy, or even nonexistent, top quark. Finally, in forming a spin-1/2 object from three fundamental spin-1/2 particles, one finds that there are two such doublets and they are independent. This opens the possibility of an even more dramatically unified model in which, starting from the same basic ur-quarks, one of the doublets is identified with the quark and the other with the corresponding lepton family.

## REFERENCES AND NOTES


1. U. Fano, in *Atomic Physics 1*, B. Bederson, V. W. Cohen, F. M. J. Pichanik, Eds. (Plenum, New York, 1969), pp. 209–225.
2. _____, *Rep. Prog. Phys.* **46**, 97 (1983).

3. P. G. Harris *et al.*, *Phys. Rev. Lett.* **65**, 309 (1990); *Phys. Rev. A* **42**, 6443 (1990).
4. M. Halka *et al.*, *Phys. Rev. A* **44**, 6127 (1991).
5. A good example is the very neutron-rich $^6$He. States with two loosely bound neutrons outside an $\alpha$ particle structure are analogs of doubly excited states. These have recently been of interest because $\beta$ decay of one of the outer neutrons (n) leads to ($\alpha$ + d) (where d is a deuteron) structures, in addition to an established $\beta$ decay of $^6$He to $^6$Li [K. Riisager *et al.*, *Phys. Lett. B* **235**, 30 (1990)]. Another neutron-rich species is $^{11}$Li, which behaves like $^9$Li + (nn) [L. Johannsen, A. S. Jensen, P. G. Hansen, *ibid.* **244**, 357 (1990); W. R. Gibbs and A. C. Hayes, *Phys. Rev. Lett.* **67**, 1395 (1991)]. Alongside their presence in such weakly bound nuclei, dineutron (nn) clusters also figure in breakup processes such as $^6\mathrm{H} \rightarrow {}^3\mathrm{H} + \mathrm{n} + (\mathrm{nn})$ and $^8\mathrm{He} \rightarrow {}^6\mathrm{He} + (\mathrm{nn})$ [K. K. Seth and B. Parker, *Phys. Rev. Lett.* **66**, 2448 (1991)]. Together, these data show that, although the dineutron is unbound by 70 keV in free space, it appears as a loosely bound pair in the field of a nucleus to which it can be loosely and temporarily attached [A. B. Migdal, *Sov. J. Nucl. Phys.* **16**, 238 (1973)].
6. J. L. Rosner and M. Worah, *Phys. Rev. D* **46**, 1131 (1992).
7. U. Fano and A. R. P. Rau, *Atomic Collisions and Spectra* (Academic Press, New York, 1986), chap. 10.
8. H. A. Bethe and E. E. Salpeter, *Quantum Mechanics of One and Two Electron Atoms* (Springer-Verlag, Berlin, 1957), section 26.
9. In heavier atoms, the lowest states of the $N = 2$ family may lie below the $N = 1$ ionization threshold, in which case autoionization decay is energetically forbidden for these states. Typical examples occur in the heavier alkaline earths such as Ca, Sr, and Ba.
10. See, for instance, C. G. Wohl *et al.*, Particle Data Group, *Rev. Mod. Phys.* **56**, S1 (1984), p. S43 and appendix I.
11. M. Kobayashi and K. Maskawa, *Prog. Theor. Phys.* **49**, 652 (1983).
12. J. L. Rosner, *Boulder TASI* **90**, 91 (1990).
13. R. P. Madden and K. Codling, *Phys. Rev. Lett.* **10**, 516 (1963).
14. P. R. Woodruff and J. A. R. Samson, *Phys. Rev. A* **25**, 848 (1982).
15. M. C. Domke *et al.*, *Phys. Rev. Lett.* **66**, 1306 (1991).
16. L. A. Bloomfield, R. R. Freeman, W. E. Cooke, J. Bokor, *ibid.* **53**, 2234 (1984).
17. P. Camus *et al.*, *ibid.* **62**, 2365 (1989); U. Eichmann, V. Lange, W. Sandner, *ibid.* **68**, 21 (1992).
18. N. Morita and T. Suzuki, *J. Phys. B.* **21**, L439 (1988).
19. H. C. Bryant *et al.*, *Phys. Rev. Lett.* **38**, 228 (1977); in *Atomic Physics 7*, D. Kleppner and F. M. Pipkin, Eds. (Plenum, New York, 1981), pp. 29–63.
20. G. J. Schulz, *Phys. Rev. Lett.* **10**, 104 (1963).
21. S. J. Buckman and D. S. Newman, *J. Phys. B* **20**, L711 (1987).
22. S. Tsurubuchi *et al.*, *ibid.* **15**, L733 (1982).
23. P. B. Cattin *et al.*, *ibid.* **21**, 3387 (1988).
24. The quantum numbers are unchanged for "allowed" autoionization decays proceeding through the $e^2/r_{12}$ interaction. In certain situations, where no such decay is possible, decay may take place through the additional help of weaker interactions such as spin-orbit or spin-spin forces between electrons. All these interactions are still scalar and of even parity so that also for these suppressed decays $J$ and $\pi$ do not change even when $S$ and $L$ may. A striking example is provided by the $1s\,2s\,2p\,^4P_{5/2}{}^o$ state of $He^-$ or Li, which can only decay to the underlying $1s^2Ef\,^2F_{5/2}{}^o$ continuum through the mediation of spin-spin interactions. Such a state is very long-lived, so much so that beams of $He^-$ in this state that live long enough to traverse the length of a laboratory can be made and studied.
25. Z. Albrecht *et al.*, ARGUS Collaboration, *Phys. Lett. B* **234**, 409 (1990).
26. L. Lipsky, R. Anania, M. J. Conneely, *At. Data Nucl. Data Tables* **20**, 727 (1977).
27. Y. K. Ho and J. Callaway, *Phys. Rev. A* **27**, 1887 (1983); *ibid.* **34**, 4402 (1986)
28. Y. K. Ho, *ibid.* **35**, 2035 (1987); *ibid.* **41**, 1492 (1990).
29. C. A. Nicolaides and Y. Komninos, *ibid.* **35**, 999 (1987); M. Chrysos, Y. Komninos, Th. Mercouris, C. A. Nicolaides, *ibid.* **42**, 2634 (1990).
30. G. Ezra, K. Richter, G. Tanner, D. Wintgen, *J. Phys. B* **24**, L413 (1991).
31. J. Feagin and J. S. Briggs, *Phys. Rev. Lett.* **57**, 984 (1986); *Phys. Rev. A* **37**, 4599 (1988).
32. J. M. Rost and J. S. Briggs, *J. Phys. B* **21**, L233 (1988); *ibid.* **22**, 3587 (1989); *ibid.* **24**, 4293 (1991).
33. J. Feagin, in *Fundamental Processes in Atomic Dynamics*, J. S. Briggs, Ed. (Plenum, New York, 1988), pp. 275–300.
34. X. H. Liu, Z. Chen, C. D. Lin, *Phys. Rev. A* **44**, 5468 (1991).
35. L. D. Landau and E. M. Lifshitz, *Quantum Mechanics: Non-Relativistic Theory* (Pergamon, Oxford, 1977), section 37.
36. J. M. Rost, J. S. Briggs, J. Feagin, *Phys. Rev. Lett.* **66**, 1642 (1990); A. Vollweiter, J. M. Rost, J. S. Briggs, *J. Phys. B* **24**, L155 (1991).
37. J. H. Macek, *J. Phys. B* **1**, 831 (1968).
38. C. D. Lin, *Phys. Rev. Lett.* **35**, 1150 (1975); *Adv. At. Mol. Phys.* **22**, 77 (1986).
39. J. H. Bartlett, *Phys. Rev.* **51**, 661 (1937); V. Fock, *K. Nor. Vidensk. Selsk. Forh.* **31**, 138 (1958).
40. A. R. P. Rau, in *Atomic Physics 9*, R. S. Van Dyck and E. N. Fortson, Eds. (World Scientific, Singapore, 1985), pp. 491–504; in *Atoms in Unusual Situations*, J. P. Briand, Ed. (Plenum, New York, 1986), pp. 383–395.
41. G. H. Wannier, *Phys. Rev.* **90**, 817 (1953).
42. H. R. Sadeghpour and C. H. Greene, *Phys. Rev. Lett.* **65**, 313 (1990).
43. D. R. Herrick, *Phys. Rev. A* **12**, 413 (1975).
44. M. Gailitis and R. Damburg, *Proc. Phys. Soc. London* **82**, 192 (1963).
45. H. R. Sadeghpour, *Phys. Rev. A* **43**, 5821 (1991).
46. _____, C. H. Greene, M. Cavagnero, *ibid.* **45**, 1587 (1992).
47. F. H. Read, *Aust. J. Phys.* **35**, 475 (1982); A. R. P. Rau, *J. Phys. B* **16**, L699 (1983).
48. This picture of the lowest doubly excited states of each family in Fig. 1 as built up of a single entity, a correlated atomic electron pair that is attached to a grandparental positive ion, has interesting similarities and dissimilarities with other pairing phenomena, such as in the interacting boson model of nuclear physics [F. Iachello, *Interacting Bosons in Nuclear Physics* (Plenum, New York, 1979)] or the Cooper pair in superconductivity [J. R. Schrieffer, *Theory of Superconductivity* (Benjamin/Cummings, Redwood City, CA, 1964), section 2.2]. In these latter problems, the pairing interaction is attractive and, therefore, a distinguished state with the tightest correlation appears as the ground state of the system, separated by a finite gap from the rest of the spectrum. In the case of doubly excited states, the interaction $e^2/r_{12}$ is repulsive and the tightest correlation appears instead at the opposite end of the spectrum, namely, the double-ionization threshold, which lies at the $N \rightarrow \infty$ limit of Fig. 1. The sequence formed by the lowest states of each family terminates at this ionization limit in the so-called Wannier threshold state (*7, 41*) that describes the escape to infinity of a pair of electrons. Radial and angular correlations are at their extreme in this Wannier state (*40*).


49. Careful reading of this manuscript by J. Briggs and M. Inokuti is appreciated, and also a useful discussion with J. Rosner. The current form of presentation also owes much to detailed suggestions and corrections by U. Fano, and his help is gratefully acknowledged. This work was supported by the National Science Foundation.


# Managing Insect Resistance to *Bacillus thuringiensis* Toxins


William H. McGaughey and Mark E. Whalon



*Bacillus thuringiensis* (*B.t.*) δ-endotoxins provide an alternative to chemical insecticides for controlling many species of pest insects. Recent biotechnological developments offer the promise of even greater use of *B.t.* toxins in genetically transformed pest-resistant crops. However, the discovery that insects can adapt to these toxins raises concerns about the long-term usefulness of *B.t.* toxins. Several methods for managing the development of resistance to *B.t.* toxins have been suggested, but none of these approaches offer clear advantages in all situations.


Insecticide resistance is a formidable complication of the use of chemical insecticides. Recently, several common species of pest insects have evolved resistance to *Bacillus thuringiensis* (*B.t.*) δ-endotoxins, indicating that biological pesticides can suffer the same fate. Although *B.t.* genes are currently used to transform plants in order to impart pest resistance in several major crops (*1–3*), the value of this approach could be seriously diminished by widespread development of resistance to *B.t.* toxins. Continued reliance on chemical insecticides might thus be necessary (*4*).


W. H. McGaughey is at the U.S. Grain Marketing Research Laboratory, Agricultural Research Service, U S. Department of Agriculture, 1515 College Avenue, Manhattan, KS 66502. M. E. Whalon is at the Department of Entomology and Pesticide Research Center, Michigan State University, East Lansing, MI 48824.


## *B.t.* in Pest Management

*Bacillus thuringiensis* is an aerobic, Gram-positive, spore-forming bacterium found commonly in the environment. It produces a number of insect toxins, the most distinctive of which are protein crystals formed during sporulation (*5*). These crystalline protein inclusions, or δ-endotoxins, are the principal active ingredients in *B.t.* formulations currently in use. The genes encod-